

Strong and electromagnetic decays of the light scalar mesons interpreted as tetraquark states

Francesco Giacosa

*Institut für Theoretische Physik
Universität Frankfurt
Johann Wolfgang Goethe - Universität
Max von Laue-Str. 1
60438 Frankfurt, Germany*

Abstract

The study of two-pseudoscalar and two-photon decays for the scalar meson nonet below 1 GeV is performed within an effective approach in which the scalar resonances are described as (Jaffe's) tetraquark states. The dominant (fall apart decay) and the subdominant (one transverse gluon as intermediate state) decay amplitudes are systematically taken into account. The latter improves the agreement with the experimental data. Possible scenarios concerning the scalar-isoscalar mixing are discussed.

1 Introduction

The interpretation of the mesonic scalar states below 2 GeV is not yet univocal established [1, 2, 3]. According to the most popular scenario, one interprets the isovector and isotriplet resonances $a_0(1400)$ and $K(1430)$ as the ground-state quark-antiquark bound states. The three isoscalar resonances $f_0(1300)$, $f_0(1500)$ and $f_0(1710)$ are a mixture of two isoscalar quarkonia and bare glueball configurations (we refer to [1, 2, 4, 5, 6, 7, 8, 9] and Refs. therein). As a consequence, the scalar states below 1 GeV (σ , k , $f_0(980)$ and $a_0(980)$) must be something else, like (loosely bound) mesonic molecular states [10, 11] or Jaffe’s tetraquark states [1, 12, 13, 14]. In this work we explore by means of an effective approach the phenomenological implications of Jaffe’s states, whose building blocks are a diquark (q^2) and an antidiquark (\bar{q}^2); calculations based on one-gluon exchange support a strong attraction among two quarks in a color antitriplet ($\bar{\mathbf{3}}_C$), a flavor antitriplet ($\bar{\mathbf{3}}_F$) and spinless configuration [1, 12] (color and flavor triplets are realized for an antidiquark). Naively speaking, a diquark ‘behaves like an antiquark’ from a flavor (and color) point of view [13]:

$$[u, d] \leftrightarrow \bar{s}, [u, s] \leftrightarrow \bar{d}, [d, s] \leftrightarrow \bar{u}, \quad (1)$$

therefore out of a diquark and an antidiquark one can build a full scalar nonet, whose most appealing property is the reversed mass-order, thus explaining the (almost) degeneracy of the isoscalar state $f_0(980)$ (whose dominant contribution is the tetraquark structure “ $\bar{s}s(\bar{u}u + \bar{d}d)$ ”) and the isovector $a_0(980)$ (the neutral one interpreted as “ $\bar{s}s(\bar{u}u - \bar{d}d)$ ”); the σ (dominantly “ $\bar{u}u\bar{d}d$ ”) is then the lightest, in between one expects the kaonic state $k(800)$ (k^+ interpreted as “ $\bar{d}d\bar{s}u$ ”), which is omitted in the compilation of PDG [15], but listed in many recent theoretical and experimental works ([16, 17, 18, 19, 20, 21, 22, 23] and Refs. therein).

Evidence for a broad σ state is also found, together with $a_0(980)$ and $f_0(980)$, in the theoretical work of [24, 25] where a unitarized ChPT is used; as shown in [26, 28] a broad scalar state k exists as well. The fact that a full scalar nonet is generated within the same approach points to a similar inner structure of the low-lying scalar states. Furthermore, the large- N_c behavior of the light scalar states indicates large non- $\bar{q}q$ amounts in their spectroscopic wave function [27, 28]. Support for the Jaffe’s states has also been found in Lattice calculations [29, 30], where the diquark q^2 and the antidiquark \bar{q}^2 are connected by a flux tube.

In [31, 32] the scalar states below 1 GeV have also a dominant tetraquark structure; mixing among light tetraquark states and heavy quarkonia states, generating two scalar nonet of mixed states below and above 1 GeV is described.

In the present work we intend to analyze the two-pseudoscalar decays of the scalar states below 1 GeV when interpreted as Jaffe’s tetraquark states; to this end we consider the dominant and the subdominant diagrams in the large- N_c expansion which describe the transition of a tetraquark scalar state into two pseudoscalars [12, 14].

The dominant diagram, depicted in Fig. 1.a, occurs by switch of a quark belonging to the compact diquark with an antiquark of the anti-diquark, thus generating two $\bar{q}q$ objects, which separate as pseudoscalar mesons: $q^2\bar{q}^2 \rightarrow (q\bar{q})(q\bar{q}) \rightarrow (q\bar{q}) + (q\bar{q})$. The two pseudoscalar mesons fall apart from the tetraquark configuration; this decay mechanism was denoted as OZI-superallowed in Ref. [12].

The subdominant diagram, depicted in Fig. 1.b, occurs via an annihilation of a quark and an antiquark (into one gluon), with subsequent $\bar{q}q$ creation and two-pseudoscalar decay: $q^2\bar{q}^2 \rightarrow qg\bar{q} \rightarrow (q\bar{q}) + (q\bar{q})$. Although suppressed by a factor N_c , the fact that the annihilation of the quark-antiquark pair can occur with only one gluon as intermediate state (as already noted in Ref. [12]), i.e. to order α_s only, may indeed indicate that the corresponding amplitudes are not negligible.

In Ref. [12] the subdominant coupling has not been considered in the decay rates; in [14] it has been introduced as the last step of the analysis in order to improve the results of the superallowed decays. In the present work we intend to systematically write down the expressions for all scalar-to-pseudoscalars transition amplitudes as functions of the strengths of the dominant ("fall apart") and subdominant ("one intermediate gluon") diagrams, denoted as c_1 and c_2 respectively. Then, by a fitting procedure to experimental known branching ratios, we determine the quantity c_2/c_1 , which measures the intensity of the subdominant decay mechanism with respect to the dominant one. Two possible solutions with a non-zero value of the ratio c_2/c_1 are discussed, which in turn correspond to different isoscalar mixing configurations.

An interesting feature of the subdominant decay is the strong enhancement of the coupling $g_{f_0 \rightarrow \bar{K}K}^2$ with respect to $g_{a_0 \rightarrow \bar{K}K}^2$, thus possibly solving the problem of Jaffe's model mentioned in [21] at the leading (OZI-superallowed, Fig. 1.a) order for which $g_{f_0 \rightarrow \bar{K}K}^2/g_{a_0 \rightarrow \bar{K}K}^2 = 1$ (if no isoscalar mixing occurs, even smaller if mixing is introduced), in clear contrast with the result $g_{f_0 \rightarrow \bar{K}K}^2/g_{a_0 \rightarrow \bar{K}K}^2 = 2.15 \pm 0.40$ reported in the analysis of Refs. [21, 22]. The subdominant decay mechanism of Fig. 1.b can explain the experimental value without introducing explicit $\bar{K}K$ clouds dressing the scalar resonances.

We then turn our attention to the decay of scalar states into two photons, which in line of the previous discussion is described by two decay mechanisms; they are analogous to the strong decay diagrams of Fig. 1, where one replaces the two pseudoscalar mesons in the final state with two photons. We present the theoretical ratios and the phenomenological discussion.

The paper is organized as follows: in section 2 we write down the Lagrangian for the description of the scalar mesons below 1 GeV as tetraquark states; the mass term and the two-body strong decays are presented. In section 3 we perform a phenomenological study with the available experimental data. In section 4 we describe the two-photon transitions and in section 5 we drive our conclusions.

2 The model

2.1 The Lagrangian

The basic terms are the pseudoscalar fields, collected in the matrix $\mathcal{P} = \frac{1}{\sqrt{2}} \sum_{i=0}^8 P^i \lambda_i$ (the λ_i are Gell-Mann matrices), and low-lying scalar fields, collected in the matrix \mathcal{S} defined as (see Appendix A):

$$\begin{aligned} \mathcal{S} &= \begin{pmatrix} \sigma_B & k^0 & k^+ \\ \bar{k}^0 & \sqrt{\frac{1}{2}}(f_B + a_0^0) & a_0^+ \\ k^- & a_0^- & \sqrt{\frac{1}{2}}(f_B - a_0^0) \end{pmatrix} \\ &= \begin{pmatrix} \frac{1}{2}[u, d][\bar{u}, \bar{d}] & \frac{1}{2}[u, d][\bar{u}, \bar{s}] & \frac{1}{2}[u, d][\bar{d}, \bar{s}] \\ \frac{1}{2}[u, s][\bar{u}, \bar{d}] & \frac{1}{2}[u, s][\bar{u}, \bar{s}] & \frac{1}{2}[u, s][\bar{d}, \bar{s}] \\ \frac{1}{2}[d, s][\bar{u}, \bar{d}] & \frac{1}{2}[d, s][\bar{u}, \bar{s}] & \frac{1}{2}[d, s][\bar{d}, \bar{s}] \end{pmatrix}, \end{aligned} \quad (2)$$

where in the second matrix the diquark-antidiquark decomposition has been made explicit. The states $\sigma_B = \frac{1}{2}[u, d][\bar{u}, \bar{d}]$ and $f_B = \frac{1}{2\sqrt{2}}([u, s][\bar{u}, \bar{s}] + [d, s][\bar{d}, \bar{s}])$ refer to *bare* (unmixed) states. A mixing of these configurations, leading to the physical states σ and $f_0(980)$, is possible and considered below.

The Lagrangian for the scalar-pseudoscalar interaction reads:

$$\begin{aligned} \mathcal{L} &= \left\langle \frac{1}{2}(\partial_\mu \mathcal{P})^2 - \mathcal{P}^2 \chi_P \right\rangle + \mathcal{L}_{mix}^P + \left\langle \frac{1}{2}(\partial_\mu \mathcal{S})^2 - \mathcal{S}^2 \chi_S \right\rangle + \mathcal{L}_{mix}^S \\ &\quad + c_1 \mathcal{S}_{ij} \langle A^i \mathcal{P}^t A^j \mathcal{P} \rangle - c_2 \mathcal{S}_{ij} \langle A^i A^j \mathcal{P}^2 \rangle, \end{aligned} \quad (3)$$

where $\langle \dots \rangle$ denotes trace over flavor. Some comments are in order:

- In the first term the quantity $\chi_P = B \cdot \text{diag}\{m_u, m_d = m_u, m_s\}$ encodes flavor symmetry violation. It corresponds to the lowest order chiral perturbation theory result [33] (see also [34] and Refs. therein), to which we refer for a careful description. The second term $\mathcal{L}_{mix}^P = -\frac{\gamma_P}{2}(P^0)^2 - z_P P^0 P^8$ takes into account the enhanced flavor-singlet mass ($U_A(1)$ anomaly) and the octet-singlet mixing, leading to the physical states (we follow the notations of [9])

$$\eta = P^8 \cos \theta_P - P^0 \sin \theta_P, \quad \eta' = P^8 \sin \theta_P + P^0 \cos \theta_P, \quad (4)$$

where θ_P is the pseudoscalar mixing angle. According to the the standard procedure [35, 36, 37] we diagonalize the corresponding η^0 - η^8 mass matrix to obtain the masses of η and η' . By using $M_\pi = 139.57$ MeV, $M_K = 493.677$ MeV (the physical charged pion and kaon masses), $M_\eta = 547.75$ MeV and $M_{\eta'} = 957.78$ MeV the mixing angle is determined as $\theta_P = -9.95^\circ$, which corresponds to the tree-level result (see details in Ref. [37]). Correspondingly one finds $M_{P^0} = \sqrt{(M_\pi^2 + 2M_K^2)}/3 + \gamma_P = 948.10$ MeV and $z_P = -0.105$ GeV² [9].

- The third and the fourth terms of Eq. (3) refer to the quadratic part of the scalar tetraquark nonet; $\chi_S = \text{diag}\{\alpha, \beta, \beta\}$ and $\alpha < \beta$ takes into account that the

diquark $[u, d]$ is lighter than the partners (due to $m_u = m_d < m_s$). In this way the masses are given as

$$M_{a_0}^2 = M_{f_B}^2 = 2\beta, \quad M_k^2 = (\alpha + \beta), \quad M_{\sigma_B}^2 = 2\alpha, \quad (5)$$

corresponding to the reversed mass ordering. The fourth term \mathcal{L}_{mix}^S describes the mixing of σ_B and f_B ; details about it are presented in the next subsection.

It is interesting to note that the same (inverted) mass ordering for the light scalars can be obtained in the framework of the $SU(3)$ linear σ model [38] with $U_A(1)$ -anomaly.

It is important to stress that in this work we consider only tree-level expression for the decays (see Sections 2.3 and 3) and no mass-shift via loop diagrams is calculated; the Lagrangian-masses for the state $a_0(980)$ and k reported in Eq. (5) (derived from the Lagrangian (3)) are therefore the physical masses in our phenomenological approach. Similarly, M_{f_B} and M_{σ_B} of Eq. (5) would be physical masses if no isoscalar mixing among σ_B and f_B would occur. The physical masses for the states σ and $f_0(980)$ are determined in the next subsection when isoscalar mixing is considered.

- The last two terms of Eq. (3) correspond to the large- N_c dominant (proportional to c_1) and subdominant (proportional to c_2) two-pseudoscalar decays of the low-lying scalars when interpreted as tetraquark states. The matrices A^i entering in the expression (3) are the three antisymmetric real 3×3 matrices:

$$A^1 = i\lambda_2, \quad A^2 = i\lambda_5, \quad A^3 = i\lambda_7. \quad (6)$$

Both terms are $SU(3)$ -flavour invariant; the details about the transformation properties are reported in Appendix A, where also the other flavour invariant terms are listed (Eq. (40)).

We do not consider in the present work decay terms which break flavour symmetry in virtue of $\alpha \neq \beta$ (Eq. (5)). Generally flavour-breaking corrections to the decay amplitudes are not large and do not change the qualitative picture; furthermore the consideration of such terms would imply a too large number of parameters for the three-level decay amplitudes. For these reasons the consideration of such terms is beyond the goal of the present paper, but it represents a possible future development of our study.

- As described in Appendix A, the $S \rightarrow PP$ interaction term $c_3 \mathcal{S}_{ij} \langle A^i A^j \mathcal{P} \rangle \langle \mathcal{P} \rangle$ is also suppressed of a factor N_c with respect to the dominant OZI-superallowed one. It is coupled to the flavour-blind pseudoscalar configuration $\langle \mathcal{P} \rangle = \sqrt{3}P^0$, connected to the physical fields η and η' in equation (4). It can however occur with at least two intermediate transverse gluons attached to P^0 , i.e. to order α_s^2 . It's contribution is then believed to be smaller than the diagram of Fig. 1.b, which takes place at order α_s . A gluonic amount in the wave functions of the η and η' states would enhance this channel, but such an eventuality seems not to occur [39, 40, 41]. Furthermore, in the analysis of [42], where the two-pseudoscalar decays of the experimentally well-known tensor mesons are evaluated, a good description of data is obtained

without an enhanced flavor-blind channel in the pseudoscalar mesonic sector. These arguments lead us not to consider the term $c_3 \mathcal{S}_{ij} \langle A^i A^j \mathcal{P} \rangle \langle \mathcal{P} \rangle$ in the present work. According to our view, the further systematical inclusion of this term, which affects the couplings involving the η and η' mesons only, would be then necessary when the experimental knowledge on the light scalar meson sector becomes more exhaustive.

2.2 Mixing

We discuss the term \mathcal{L}_{mix}^S of Eq. (3) which generates mixing between σ_B and f_B . In line with the pseudoscalar sector we consider the flavor singlet and octet four-quark configurations $S_0 = \sqrt{2/3}f_B + \sqrt{1/3}\sigma_B$ and $S_8 = \sqrt{1/3}f_B - \sqrt{2/3}\sigma_B$ and define

$$\mathcal{L}_{mix}^S = -\frac{1}{2}\gamma_S S_0^2 - z_S S_0 S_8, \quad (7)$$

where a octet-singlet mixing and mass-modification for the flavor blind state are taken into account; we also refer to [14] for this point.

By using Eqs. (3) and (7) the quadratic part referring to the isoscalar states f_B and σ_B and their relative mixing reads:

$$\mathcal{L}_{isoscalar}^S = -\frac{1}{2} \begin{pmatrix} \sigma_B & f_B \end{pmatrix} \Omega \begin{pmatrix} \sigma_B \\ f_B \end{pmatrix}, \quad (8)$$

where

$$\Omega = \begin{pmatrix} M_{\sigma_B}^2 & \varepsilon \\ \varepsilon & M_{f_B}^2 \end{pmatrix} = \begin{pmatrix} 2\alpha + \frac{1}{3}\gamma_S - \frac{2\sqrt{2}}{3}z_S & -\frac{1}{3}z_S + \frac{\sqrt{2}}{3}\gamma_S \\ -\frac{1}{3}z_S + \frac{\sqrt{2}}{3}\gamma_S & 2\beta + \frac{2}{3}\gamma_S + \frac{2\sqrt{2}}{3}z_S \end{pmatrix} \quad (9)$$

(note that $M_{\sigma_B}^2$ and $M_{f_B}^2$ receive extra-contributions from (7) and therefore modified from Eq. (5)).

The physical states σ and $f_0 \equiv f_0(980)$ are then given by

$$\begin{pmatrix} \sigma \\ f_0(980) \end{pmatrix} = \begin{pmatrix} \cos(\theta_S) & \sin(\theta_S) \\ -\sin(\theta_S) & \cos(\theta_S) \end{pmatrix} \begin{pmatrix} \sigma_B \\ f_B \end{pmatrix} \quad (10)$$

where

$$B = \begin{pmatrix} \cos(\theta_S) & \sin(\theta_S) \\ -\sin(\theta_S) & \cos(\theta_S) \end{pmatrix}, \quad B\Omega B^t = \text{diag}\{M_\sigma^2, M_{f_0}^2\}. \quad (11)$$

The experimental fact that $M_{f_0} \simeq M_{a_0}$ suggests a small scalar mixing angle θ_S . Unfortunately, to determine θ_S from the masses can be misleading because of the large widths of k and σ . Furthermore, small variation of the a_0 and f_0 masses and mixing can lead to different scenarios. We therefore prefer to determine the mixing angle from the decay amplitudes (see section 4).

Nevertheless some interesting considerations can be done; exploiting the relation $\langle \Omega \rangle = M_\sigma^2 + M_{f_0}^2$ (from Eq. (11); the matrix B is orthogonal) one finds $\gamma_S =$

$M_{f_0}^2 + M_\sigma^2 - 2 \cdot M_k^2$. The sign of γ_S strongly depends on the values of M_σ and M_k . One has then to tune the parameter z_S in order to generate the experimental value $M_{f_0} = M_{a_0} \simeq 0.98$ GeV, then the mixing angle θ_S is also fixed¹. We then distinguish among 2 possibilities:

- a) $\gamma_S > 0 \rightarrow z_S < 0$ and $\theta_S < 0$; in the upper state f_0 the bare components σ_B and f_B are in phase, while in the lower state σ they are out of phase.
- b) $\gamma_S < 0 \rightarrow z_S > 0$ and $\theta_S > 0$; the phases are reversed.

The sign of θ_S is important because of destructive or constructive interference phenomena in the decays of σ and f_0 . However, as stressed above, it cannot be determined from the knowledge of the masses because of the large uncertainties on their values. We consider two examples to elucidate this point. Fixing $M_k = 0.8$ GeV, we have $\gamma_S > 0$ (and $\theta_S < 0$) for $M_\sigma > 0.56$ GeV; vice versa for $M_\sigma < 0.56$ one has $\gamma_S < 0$ (and $\theta_S > 0$). Small changes of M_k generate very different result; fixing $M_k = 0.72$ (the pole of E791 [19]) one finds $\gamma_S > 0$ (and $\theta_S < 0$) for $M_\sigma > 0.277$ GeV (therefore, if $M_k \sim 0.7$ GeV the option $\theta_S < 0$ seems favoured). We notice that the present results differ from those of [14].

In Section 4 we will determine the values of the scalar mixing angle θ_S from the phenomenology and discuss the implications for the masses.

2.3 Two-pseudoscalar decay amplitudes

In the following we report the results for the two-pseudoscalar decay rates. We use the following notation: for a given decay mode $S \rightarrow P_1 P_2$ (where S refers to a scalar state and $P_1(P_2)$ to a pseudoscalar state) the decay width (for kinematically allowed decays) is written as

$$\Gamma_{S \rightarrow P_1 P_2} = \frac{p_{S \rightarrow P_1 P_2}}{8\pi M_S^2} g_{S \rightarrow P_1 P_2}^2, \quad (12)$$

where $p_{S \rightarrow P_1 P_2}$ is the three-momentum of (one of) the outgoing particle(s) (in the rest frame of S):

$$p_{S \rightarrow P_1 P_2} = \frac{1}{2M_S} \sqrt{M_S^4 + (M_{P_1}^2 - M_{P_2}^2)^2 - 2(M_{P_1}^2 + M_{P_2}^2)M_S^2}. \quad (13)$$

Notice that $g_{S \rightarrow P_1 P_2}^2$ already includes the charge multiplicities and the symmetry factors (see Appendix B).

In general, but especially when $M_S < M_{P_1} + M_{P_2}$, the expression (12) has to be modified taking into account the finite width of the resonance, thus integrating over the mass of the resonance by employing a suitable mass distribution (like a Breit-Wigner one). However, the expressions for the coupling constant are left invariant

¹The parameter z_S can be found from $Det[\Omega] = M_\sigma^2 \cdot M_{f_0}^2$ (see Eq. (11)). Indeed, this is a second order equation in z_S , so strictly speaking two solutions are possible. The solution corresponding to the smallest absolute value $|\theta_S|$ is the one that we take into account. The disregarded solution typically induces a very large mixing, in disagreement with the phenomenology (see Section 4).

by these operations. We refer to Appendix B for a brief recall on the connection between Eq. (12) and the Lagrangian (3).

In Table 1 we list the coupling constants for the isovector $a_0(980)$ and the isodoublet(s) k to two pseudoscalar mesons as function of the dominant and subdominant decay strengths c_1 and c_2 . The expressions in $\{\dots\}$ represent the invariant amplitudes, eventually multiplied by a factor 2 for decays into identical particles, while the coefficients in front of the parenthesis account for charge multiplicities and symmetry factors (see Appendix B).

In Table 2 we report the results for the bare states σ_B and f_B ; although not physical when $\theta_S \neq 0$, the expressions are easier to read and allow to understand the role of the subleading decay mechanism of Fig. 1.b. It is important to note that the decay mode $f_B \rightarrow \overline{K}K$ is significantly enhanced with respect to $a_0 \rightarrow \overline{K}K$ when $c_2/c_1 > 0$. This fact shows that a non-negligible and positive ratio c_2/c_1 can explain why the $f_0 \rightarrow \overline{K}K$ coupling is larger than the $a_0 \rightarrow \overline{K}K$ one. This point will be discussed in the next Section.

When considering the mixed physical states σ and $f_0(980)$ defined in Eq. (10) the coupling constants are modified as follows:

$$\begin{aligned} g_{\sigma \rightarrow P_1 P_2} &= \{g_{\sigma_B \rightarrow P_1 P_2} \cdot \cos(\theta_S) + g_{f_B \rightarrow P_1 P_2} \cdot \sin(\theta_S)\} \\ g_{f_0 \rightarrow P_1 P_2} &= \{-g_{\sigma_B \rightarrow P_1 P_2} \cdot \sin(\theta_S) + g_{f_B \rightarrow P_1 P_2} \cdot \cos(\theta_S)\} \end{aligned} \quad (14)$$

Because of their relevance, we report in Table 3 the explicit expressions for the decays of σ and $f_0(980)$ into $\pi\pi$ and $\overline{K}K$ as derived from Table 2 and Eqs. (14).

Table 1. Decay coupling constants for a_0 and k

$S \rightarrow P_1 P_2$	$g_{S \rightarrow P_1 P_2}$
$a_0 \rightarrow \overline{K}K$	$\sqrt{2} \cdot \left\{ \sqrt{2}c_1 + \frac{1}{\sqrt{2}}c_2 \right\}$
$a_0 \rightarrow \pi\eta$	$\sqrt{1} \cdot \left\{ \frac{2}{\sqrt{3}}c_1 [\sqrt{2}\cos(\theta_P) + \sin(\theta_P)] + \sqrt{\frac{2}{3}}c_2 [\cos(\theta_P) - \sqrt{2}\sin(\theta_P)] \right\}$
$a_0 \rightarrow \pi\eta'$	$\sqrt{1} \cdot \left\{ -\frac{2}{\sqrt{3}}c_1 [\cos(\theta_P) - \sqrt{2}\sin(\theta_P)] + \sqrt{\frac{2}{3}}c_2 [\sqrt{2}\cos(\theta_P) + \sin(\theta_P)] \right\}$
$k \rightarrow \pi K$	$\sqrt{3} \cdot \left\{ \sqrt{2}c_1 + \frac{1}{\sqrt{2}}c_2 \right\}$
$k \rightarrow K\eta$	$\sqrt{1} \cdot \left\{ -\sqrt{\frac{2}{3}}c_1 [\cos(\theta_P) - \sqrt{2}\sin(\theta_P)] - \sqrt{\frac{1}{6}}c_2 [\cos(\theta_P) + 2\sqrt{2}\sin(\theta_P)] \right\}$
$k \rightarrow K\eta'$	$\sqrt{1} \cdot \left\{ -\sqrt{\frac{2}{3}}c_1 [\sqrt{2}\cos(\theta_P) + \sin(\theta_P)] + \sqrt{\frac{1}{6}}c_2 [2\sqrt{2}\cos(\theta_P) - \sin(\theta_P)] \right\}$

Table 2. Decay coupling constants of the bare states σ_B and f_B

$S \rightarrow P_1 P_2$	$g_{S \rightarrow P_1 P_2}$
$\sigma_B \rightarrow \pi\pi$	$\sqrt{\frac{3}{2}} \cdot \{2c_1 + 2c_2\}$
$\sigma_B \rightarrow \bar{K}K$	$\sqrt{2} \cdot \{c_2\}$
$\sigma_B \rightarrow \eta\eta$	$\sqrt{\frac{1}{2}} \cdot \left\{ \frac{2}{3}(-c_1 + c_2) (\cos(\theta_P) - \sqrt{2} \sin(\theta_P))^2 \right\}$
$\sigma_B \rightarrow \eta'\eta'$	$\sqrt{\frac{1}{2}} \cdot \left\{ \frac{2}{3}(-c_1 + c_2) (\sqrt{2} \cos(\theta_P) + \sin(\theta_P))^2 \right\}$
$\sigma_B \rightarrow \eta\eta'$	$\sqrt{1} \cdot \left\{ \frac{1}{3}(-c_1 + c_2) (2\sqrt{2} \cos(2\theta_P) - \sin(2\theta_P)) \right\}$
$f_B \rightarrow \pi\pi$	$\sqrt{\frac{3}{2}} \cdot \{\sqrt{2}c_2\}$
$f_B \rightarrow \bar{K}K$	$\sqrt{2} \cdot \left\{ \left(\sqrt{2}c_1 + \frac{3}{\sqrt{2}}c_2 \right) \right\}$
$f_B \rightarrow \eta\eta$	$\sqrt{\frac{1}{2}} \cdot \left\{ \frac{1}{6} (9\sqrt{2}c_2 + \sqrt{2}(8c_1 + c_2) \cos(2\theta_P) + 4(-c_1 + c_2) \sin(2\theta_P)) \right\}$
$f_B \rightarrow \eta'\eta'$	$\sqrt{\frac{1}{2}} \cdot \left\{ \frac{1}{6} (9\sqrt{2}c_2 - \sqrt{2}(8c_1 + c_2) \cos(2\theta_P) + 4(c_1 - c_2) \sin(2\theta_P)) \right\}$
$f_B \rightarrow \eta\eta'$	$\sqrt{1} \cdot \left\{ \frac{1}{6} (4(c_1 - c_2) \cos(2\theta_P) + \sqrt{2}(8c_1 + c_2) \sin(2\theta_P)) \right\}$

Table 3. Decay coupling constants of the physical states σ and f_0

$S \rightarrow P_1 P_2$	$g_{S \rightarrow P_1 P_2}$
$\sigma \rightarrow \pi\pi$	$\sqrt{\frac{3}{2}} \cdot \{2c_1 \cos(\theta_S) + c_2(2 \cos(\theta_S) + \sqrt{2} \sin(\theta_S))\}$
$\sigma \rightarrow \bar{K}K$	$\sqrt{2} \cdot \left\{ \sqrt{2}c_1 \sin(\theta_S) + c_2(\cos(\theta_S) + \frac{3}{\sqrt{2}} \sin(\theta_S)) \right\}$
$f_0 \rightarrow \pi\pi$	$\sqrt{\frac{3}{2}} \cdot \{-2c_1 \sin(\theta_S) + c_2(-2 \sin(\theta_S) + \sqrt{2} \cos(\theta_S))\}$
$f_0 \rightarrow \bar{K}K$	$\sqrt{2} \cdot \left\{ \sqrt{2}c_1 \cos(\theta_S) + c_2(-\sin(\theta_S) + \frac{3}{\sqrt{2}} \cos(\theta_S)) \right\}$

3 Strong decays: numerical results

The data about the decay widths reported in [15] are still not complete. The resonance σ is very broad ($M_\sigma = 0.4-1.2$ GeV, $\Gamma = 0.6-1$ GeV), k is still not yet listed (in the recent result of [20] the pole is found at 0.76 GeV, the width is very large). The masses for the states $a_0(980)$ and $f_0(980)$ are well known, $M_{a_0} = 948.7 \pm 1.2$ MeV $M_{f_0} = 980 \pm 10$ MeV, but the widths are not, between 40 and 100 MeV for both states. The presence of near-threshold $\bar{K}K$ decays complicates the experimental and theoretical analysis (see discussion in [25, 43] and below).

Information about (some of) the coupling constants $g_{S \rightarrow P_1 P_2}^2$ has been extracted directly from experiment [20, 21, 22, 43]. In the case of $a_0(980)$, for instance, the quantities $g_{a_0 \rightarrow \pi\eta}^2$, $g_{a_0 \rightarrow \bar{K}K}^2$ and M_{a_0} are free parameters of the meson-meson scattering amplitudes (generally the Flatté distribution is used [43, 44]). They can be determined by fitting the theoretical amplitudes to the experimental ones. However, as explained in [43], relatively large differences in the absolute values of the coupling constants $g_{a_0 \rightarrow \pi\eta}^2$ and $g_{a_0 \rightarrow \bar{K}K}^2$ are found in the literature. Fortunately, the ratio $g_{a_0 \rightarrow \pi\eta}^2/g_{a_0 \rightarrow \bar{K}K}^2$ shows a stable behavior.

Furthermore, the presence of strong coupling constant for the near-threshold decay mode $g_{a_0 \rightarrow \bar{K}K}$ affects also the channel $a_0 \rightarrow \pi\eta$ rendering the experimental width narrower than the theoretical result obtained using Eq. (12), see the discussion in [25].

In the following we will compare our results with the analysis of experimental results of Refs. [20, 21, 22], where the ratios of coupling constants for various decay channels are deduced; it should be stressed that the results of [20, 21, 22] are not yet conclusive and depend on the choice of the form factors and other assumptions, for which we refer to the above cited works for a careful description.

The ratios of coupling constants for the resonances $a_0(980)$ and $f_0(980)$ as reported in [20, 21, 22] are:

$$\frac{g_{f_0 \rightarrow \bar{K}K}^2}{g_{f_0 \rightarrow \pi\pi}^2} = 4.21 \pm 0.46, \quad \frac{g_{f_0 \rightarrow \bar{K}K}^2}{g_{a_0 \rightarrow \bar{K}K}^2} = 2.15 \pm 0.40, \quad \frac{g_{a_0 \rightarrow \pi\eta}^2}{g_{a_0 \rightarrow \bar{K}K}^2} = 0.75 \pm 0.11. \quad (15)$$

These three results are indeed (at least qualitatively) common to (almost) all the analyses (see [43] and Refs. therein, and the recent experimental analysis of [45, 47]). The largest uncertainty is about the crossed ratio $g_{f_0 \rightarrow \bar{K}K}^2/g_{a_0 \rightarrow \bar{K}K}^2$; however, the enhanced coupling of the $f_0 \rightarrow \bar{K}K$ mode with respect to $a_0 \rightarrow \bar{K}K$ is also a stable result. As we will see, all three ratios in (15) are all compatible with a sizable c_2/c_1 .

Before considering a nonzero value for c_2/c_1 , we analyze as a first step the case $c_2 = 0$, corresponding to the original work of [12] and described in the recent paper of [21]. We fit the only free parameter θ_S to the first and the second branching ratios of Eq. (15); the ratio $g_{a_0 \rightarrow \pi\eta}^2/g_{a_0 \rightarrow \bar{K}K}^2 = 0.50$ does not depend on θ_S , hence not included in the fit (in [21] it is 0.4 because of a slightly different pseudoscalar mixing angle; here it is $\theta_P = -9.95^\circ$, while in [21] the value $\theta_P = -17.29^\circ$ is used).

We find the following value for θ_S (we refer to this case as Solution A):

$$\text{Sol. A: } (c_2 = 0), \quad \theta_S = \pm 21.6^\circ; \quad \left(\frac{\chi^2}{2} = 5.17\right) \quad (16)$$

corresponding to the values

$$\frac{g_{f_0 \rightarrow \bar{K}K}^2}{g_{f_0 \rightarrow \pi\pi}^2} = 4.26, \quad \frac{g_{f_0 \rightarrow \bar{K}K}^2}{g_{a_0 \rightarrow \bar{K}K}^2} = 0.86, \quad \frac{g_{a_0 \rightarrow \pi\eta}^2}{g_{a_0 \rightarrow \bar{K}K}^2} = 0.50. \quad (17)$$

The large and unsatisfactory χ^2 is generated by the mismatch between experiment and theory for the ratio $g_{f_0 \rightarrow \overline{K}K}^2/g_{a_0 \rightarrow \overline{K}K}^2$. Two scalar mixing angles are reported in Eq. (16) because the fitted quantities are symmetric for $\theta_S \rightarrow -\theta_S$ when $c_2 = 0$. Our theoretical ratio for $g_{f_0 \rightarrow \overline{K}K}^2/g_{f_0 \rightarrow \pi\pi}^2$ as function of θ_S is deduced from Table 3 and reads for $c_2 = 0$:

$$\frac{g_{f_0 \rightarrow \overline{K}K}^2}{g_{f_0 \rightarrow \pi\pi}^2} = \frac{2}{3} \cot^2(\theta_S). \quad (18)$$

We notice that in [21] the theoretical ratio is $g_{f_0 \rightarrow \overline{K}K}^2/g_{f_0 \rightarrow \pi\pi}^2 = \frac{1}{3} \cot^2(\theta_S)$; for this reason the mixing angle found in [21] is $\theta_S = \pm 15.9^\circ$ and differs from our result. The extra-factor 1/2 present in the result of [21] could not be verified when evaluating the traces of Eq. (3).

We now consider a non-zero c_2 : in principle one could determine the ratio c_2/c_1 from the quantity $g_{a_0 \rightarrow \pi\eta}^2/g_{a_0 \rightarrow \overline{K}K}^2$ alone. In fact, the theoretical expression depends only on c_2/c_1 . When $c_2 = 0$ the result as derived from Table 1 is 0.5, then $g_{a_0 \rightarrow \pi\eta}^2/g_{a_0 \rightarrow \overline{K}K}^2$ increases very slowly for increasing c_2/c_1 . The value $g_{a_0 \rightarrow \pi\eta}^2/g_{a_0 \rightarrow \overline{K}K}^2 = 0.6$ is reached when $c_2/c_1 = 0.6$, but the value $g_{a_0 \rightarrow \pi\eta}^2/g_{a_0 \rightarrow \overline{K}K}^2 = 0.75$ corresponds to $c_2/c_1 = 2.35$. Because of this strong sensibility it is not practicable to determine c_2/c_1 in this way. However, a sizable c_2 improves the agreement with the experiment.

The χ^2 -method is then used to find the free quantities c_2/c_1 and θ_S which correspond to the best description of (15) (Solution B):

$$\text{Sol. B: } c_2/c_1 = 0.62, \theta_S = -12.8^\circ; \left(\frac{\chi^2}{3} = 0.65 < 1\right). \quad (19)$$

The theoretical ratios evaluated with the parameters of Sol. B are:

$$\frac{g_{f_0 \rightarrow \overline{K}K}^2}{g_{f_0 \rightarrow \pi\pi}^2} = 4.21, \quad \frac{g_{f_0 \rightarrow \overline{K}K}^2}{g_{a_0 \rightarrow \overline{K}K}^2} = 2.28, \quad \frac{g_{a_0 \rightarrow \pi\eta}^2}{g_{a_0 \rightarrow \overline{K}K}^2} = 0.60, \quad (20)$$

thus in good agreement with the results of (15). The inclusion of the subdominant decay diagram of Fig. 1.b leads to a clear improvement of all three ratios without adding $\overline{K}K$ contributions to the wave functions of the resonances. Notice that within this Solution a negative value for the scalar mixing angle is preferred.

In [21, 22] a large ratio $g_{\sigma \rightarrow \overline{K}K}^2/g_{\sigma \rightarrow \pi\pi}^2 = 0.6 \pm 0.1$ is deduced from analysis of $\phi \rightarrow \gamma\pi^0\pi^0$ (such a large ratio can explain a problem in reproducing the overall normalizations; other explanations are however possible [48, 49]). With the parameters of Sol. B (19) one finds a very small ratio: $g_{\sigma \rightarrow \overline{K}K}^2/g_{\sigma \rightarrow \pi\pi}^2 = 4.8 \cdot 10^{-7}$. Such a small value is caused by the destructive interference between the σ_B and f_B components (see Table 3). If the value of [22] should be confirmed by future experimental analyses, our Sol. B should be rejected.

We make a second fit by adding to the data in (15) the value $g_{\sigma \rightarrow \overline{K}K}^2/g_{\sigma \rightarrow \pi\pi}^2 = 0.6 \pm 0.1$. The minimum of χ^2 is found for (Solution C):

$$\text{Sol. C: } c_2/c_1 = 0.89, \theta_S = 35.8^\circ; \left(\frac{\chi^2}{4} = 2.04\right). \quad (21)$$

The results derived from the Solutions A, B and C are summarized in Table 4, where also other coupling ratios are presented. In Sol. C a large branching ratio $\overline{K}K/\pi\pi$ for the σ resonance is found (0.65), however $g_{f_0 \rightarrow \overline{K}K}^2/g_{a_0 \rightarrow \overline{K}K}^2$ gets worse (1.12, generating a large χ^2 ; it is however still larger than 1).

Table 4. Comparison of coupling ratios with the analysis of experimental results of Refs. [21, 22] ²

Ratios of g^2	Sol. A (16)	Sol. B (19)	Sol. C (21)	Analysis of Refs. [21, 22]
$g_{a_0 \rightarrow \pi\eta}^2/g_{a_0 \rightarrow \overline{K}K}^2$	0.50	0.60	0.63	0.75 ± 0.11
$g_{f_0 \rightarrow \overline{K}K}^2/g_{f_0 \rightarrow \pi\pi}^2$	4.26	4.21	4.35	4.21 ± 0.16
$g_{f_0 \rightarrow \overline{K}K}^2/g_{a_0 \rightarrow \overline{K}K}^2$	0.86	2.28	1.11	2.15 ± 0.4
$g_{a_0 \rightarrow \pi\eta'}^2/g_{a_0 \rightarrow \pi\eta}^2$	1.01	0.16	0.05	-
$g_{f_0 \rightarrow \eta\eta}^2/g_{f_0 \rightarrow \pi\pi}^2$	1.78 (1.57)	1.35	2.30	< 0.33
$g_{\sigma \rightarrow \overline{K}K}^2/g_{\sigma \rightarrow \pi\pi}^2$	0.10	$4.8 \cdot 10^{-7}$	0.65	0.6 ± 0.1
$g_{\sigma \rightarrow \eta\eta}^2/g_{\sigma \rightarrow \pi\pi}^2$	0.30 (0.02)	0.05	0.10	0.20 ± 0.04
$g_{k \rightarrow \pi K}^2/g_{\sigma \rightarrow \pi\pi}^2$	1.16	0.78	0.58	(2.14 ± 0.28) to (1.35 ± 0.10)
$g_{k \rightarrow \eta K}^2/g_{k \rightarrow \pi K}^2$	0.17	0.12	0.11	0.06 ± 0.02
$g_{k \rightarrow \eta' K}^2/g_{k \rightarrow \pi K}^2$	0.16	0.006	~ 0	0.29 ± 0.29

Some comments are in order:

a) The first three ratios refer to $a_0(980)$ and to $f_0(980)$, which have been studied in details in the literature for what concern the $\overline{K}K$, $\pi\eta$ and $\pi\pi$ channels. For these reasons our preferred solution is Sol. B (19), which is in good agreement with these three experimental ratios.

The other ratios refer to the broad σ and k states or to channels far from threshold for a_0 and f_0 , therefore are not free of ambiguities.

b) The ratio $g_{\sigma \rightarrow \overline{K}K}^2/g_{\sigma \rightarrow \pi\pi}^2$ is the main difference between Solutions B and C, which also generates different values for the scalar angle, negative in the first case and positive in the second. We notice also a large discrepancy of all three Solutions for the branching ratio $g_{f_0 \rightarrow \eta\eta}^2/g_{f_0 \rightarrow \pi\pi}^2$, whose experimental value reported in [21] is smaller than the theoretical results for Jaffe's tetraquark states. Future checks on these two quantities may help to disentangle the nature of the light scalar mesons.

²The results for Sol. A are equal for the two mixing angles $\theta_S = \pm 21.6^\circ$, with the exception of two ratios: $g_{f_0 \rightarrow \eta\eta}^2/g_{f_0 \rightarrow \pi\pi}^2$ and $g_{\sigma \rightarrow \eta\eta}^2/g_{\sigma \rightarrow \pi\pi}^2$, for which the first result corresponds to $\theta_S = -21.6^\circ$, while the second (in parenthesis) to $\theta_S = 21.6^\circ$.

c) In Solutions *B* and *C* the ratio c_2/c_1 is not small. The inclusion of the decay mechanism of Fig. 1.b (which can occur with one gluon as intermediate state) represents an improvement for the phenomenology of Jaffe's tetraquark states. Indeed, this result has been anticipated in [14], where the quantity c_2/c_1 varies between 0.7 and 1 (for comparison, the parameters a and b in [14] are $2c_1$ and $-c_2$ in the present work).

In particular, one can notice that the first three entries of Table 4 are improved in Sol. B when compared to Sol. A (corresponding to $c_2 = 0$), thus a non-zero and sizable ratio c_2/c_1 is favoured within the here presented phenomenological analysis.

In Sol. B the ratio $c_2/c_1 = 0.62$ lies in between $1/N_c = 1/3$ and 1. Although larger than $1/3$, it is still clearly smaller than 1. Sol. B is still in agreement with expectations from large N_c considerations. In Sol. C one has $c_2/c_1 = 0.89$, which is of order 1. Such a value would imply a substantial violation from large N_c ; this fact constitutes a further hint in favor of Sol. B.

d) The coupling $g_{k \rightarrow \pi K}^2$ is smaller than $g_{\sigma \rightarrow \pi \pi}^2$ in solution *B* and *C*; this is not in accord with the experimental result describing such a wide k resonance (curiously, Solution A is better in this respect). Two experimental values are reported in Table 4 (see [21]), the second one does not represent such a large mismatch with the theoretical values. It is noticeable that a similar problem exists when describing the scalar sector above 1 GeV ([9] and Refs. therein): the experimental large width of the state $K_0(1430)$ cannot be explained theoretically.

e) The knowledge of the mixing angle does not allow us to deduce M_σ and M_k . However, we can consider reasonable values for M_σ and determine M_k for which the mixing angles of Sol. B and C are realized: if we take $M_\sigma = 0.45$ GeV, then a scalar mixing angle $\theta_S = -12.8^\circ$ (Sol. B (19)) corresponds to $M_k = 0.69$ GeV, while a mixing angle $\theta_S = 35.8^\circ$ (Sol. C (21)) to $M_k = 0.944$ GeV. Similarly, if $M_\sigma = 0.55$ GeV the corresponding couples of values ($\theta_S = -12.8^\circ, M_k = 0.735$ GeV) and ($\theta_S = 31.8^\circ, M_k = 0.953$ GeV) are found. The present values for the k pole favor a light mass between 0.7 and 0.8 GeV [19, 20], therefore Sol. B is in better agreement with the data. (However, the analysis of [46] points to a slightly heavier kaonic state: $M_k = 841 \pm 30_{-73}^{+81}$, therefore caution is still needed when driving conclusions).

f) Keeping in mind the remarks at the beginning of this section, we nevertheless discuss some full widths as (naively) calculated from Eq. (12); in [43] various values for $g_{a_0 \rightarrow \pi \eta}^2$ are reported ($= \bar{g}_\eta \cdot 8\pi M_{a_0}^2$ in [43]). The results vary between 5 and 10 GeV². We take for simplicity a value in between: $g_{a_0 \rightarrow \pi \eta}^2 = 7.5$ GeV². For Sol. B such a value corresponds to $c_1 = 1.32$ GeV, resulting in (values in MeV) $\Gamma_{f_0 \rightarrow \pi \pi} = 136$, $\Gamma_{a_0 \rightarrow \pi \eta} = 98$, $\Gamma_{\sigma \rightarrow \pi \pi} = 795$ and $\Gamma_{k \rightarrow K \pi} = 251$. For Sol. C we have $c_1 = 1.19$ GeV, implying $\Gamma_{f_0 \rightarrow \pi \pi} = 58$, $\Gamma_{a_0 \rightarrow \pi \eta} = 98$, $\Gamma_{\sigma \rightarrow \pi \pi} = 1013$ and $\Gamma_{k \rightarrow K \pi} = 241$. Clearly the widths change substantially when varying $g_{a_0 \rightarrow \pi \eta}^2$ in the mentioned range. The qualitative picture emerging is the presence in both cases of two broad states σ and k with $\Gamma_{\sigma \rightarrow \pi \pi} > \Gamma_{k \rightarrow K \pi}$ (but the latter not so broad as desired), and two narrower partial decay widths for f_0 and a_0 ; notice that the ordering $\Gamma_{f_0 \rightarrow \pi \pi} > \Gamma_{a_0 \rightarrow \pi \eta}$ in Sol.

B is reversed in Sol. C. The inclusion of a mass distribution for the calculation of the decay widths, thus also evaluating the \overline{KK} modes for a_0 and f_0 , is planned as a future step but beyond the goal of the present work.

g) Before moving to the two-photon decays, we wish to remind what has been considered and what omitted in the performed study on strong decays. The two interaction terms of the Lagrangian (3) are $SU_V(3)$ -invariant and correspond to the diagrams of Fig. 1; other flavour symmetric terms, listed in Eq. (40), and direct $SU_V(3)$ -breaking interactions have been omitted. They are supposed to represent corrections to the here presented scenario(s) (large N_c -suppressed terms and flavor symmetry breaking corrections) eventually useful for a more quantitative study. By performing a fit leading to Sol. B we used as experimental quantities the values reported in [20, 21, 22]; as already noticed above, these three results, although qualitatively similar to other works on light scalars, depend on particular assumption of form factors. Furthermore, the errors are only statistical and not systematic. Even more caution is needed with the other values reported in the right column of Table 4. Being aware of these limitations of both theoretical and experimental origin, we however intended to focus on a particular and interesting aspect of phenomenology of four-quark states encoded in the two diagrams of Fig. 1.

4 Two-photon decays

We now turn the attention to the $\gamma\gamma$ -decays of the Jaffe's tetraquark states. As for the strong decays we consider two analogous channels, where one has photons instead of mesons as final states in Fig 1. The Lagrangian reads

$$\mathcal{L}_{em} = c_1^{\gamma\gamma} \mathcal{S}_{ij} \langle A^i Q A^j Q \rangle F_{\mu\nu}^2 - c_2^{\gamma\gamma} \mathcal{S}_{ij} \langle A^i A^j Q^2 \rangle F_{\mu\nu}^2, \quad (22)$$

where $Q = e \cdot \text{diag}\{2/3, -1/3, -1/3\}$ is the charge matrix ($e = \sqrt{4\pi\alpha}$ is the electron charge, $\alpha \simeq 1/137$) and $F_{\mu\nu} = \partial_\mu A_\nu - \partial_\nu A_\mu$ the electromagnetic field tensor. Note that the convention for the relative sign of the leading and subleading terms is the same of Eq. (3) (see also Appendix A).

The decay width into two photons reads

$$\Gamma_{S \rightarrow \gamma\gamma} = 16\pi\alpha^2 M_S^3 \cdot g_{S \rightarrow \gamma\gamma}^2, \quad (23)$$

where the nonzero contributions obviously correspond to $S = a_0^0, \sigma, f_0$. The coupling constants for a_0^0 and for the bare states σ_B and f_B are deduced from (22) and read:

$$g_{a_0^0 \rightarrow \gamma\gamma} = \frac{2c_1^{\gamma\gamma} + c_2^{\gamma\gamma}}{3\sqrt{2}}, \quad g_{\sigma_B \rightarrow \gamma\gamma} = \frac{4c_1^{\gamma\gamma} + 5c_2^{\gamma\gamma}}{9}, \quad g_{f_B \rightarrow \gamma\gamma} = \frac{2c_1^{\gamma\gamma} + 7c_2^{\gamma\gamma}}{9\sqrt{2}} \quad (24)$$

When considering the mixed physical states σ and $f_0(980)$ defined in Eq. (10) the coupling constants are modified as (see also Eq. (14)):

$$\begin{aligned} g_{\sigma \rightarrow \gamma\gamma} &= g_{\sigma_B \rightarrow \gamma\gamma} \cdot \cos(\theta_S) + g_{f_B \rightarrow \gamma\gamma} \cdot \sin(\theta_S), \\ g_{f_0 \rightarrow \gamma\gamma} &= -g_{\sigma_B \rightarrow \gamma\gamma} \cdot \sin(\theta_S) + g_{f_B \rightarrow \gamma\gamma} \cdot \cos(\theta_S). \end{aligned} \quad (25)$$

The experimental results for the decay width of a_0 and f_0 are given by [15]

$$\Gamma_{f_0 \rightarrow \gamma\gamma} = 0.39_{-0.13}^{+0.10} \text{ KeV}, \Gamma_{a_0^0 \rightarrow \gamma\gamma} = 0.30 \pm 0.10 \text{ KeV}. \quad (26)$$

The experimental value for $\Gamma_{a_0^0 \rightarrow 2\gamma}$ is not reported as an average in [15]; however, it is in accord with the quoted averages $\Gamma_{a_0^0 \rightarrow 2\gamma} \cdot (\Gamma_{\eta\pi}/\Gamma_{tot}) = 0.24_{-0.07}^{+0.08} \text{ KeV}$ and $\Gamma_{\bar{K}K}/\Gamma_{\eta\pi} = 0.183 \pm 0.024$. Combining these two results one finds $\Gamma_{a_0^0 \rightarrow \gamma\gamma} = 0.28 \pm 0.10 \text{ KeV}$, well compatible with (26). In [50] it was shown that two-photon widths about 0.3 keV are compatible with a tetraquark nature of the states.

Expressing the results of (26) in terms of squared coupling constants we find

$$\frac{\Gamma_{a_0^0 \rightarrow \gamma\gamma}}{\Gamma_{f_0 \rightarrow \gamma\gamma}} = \frac{g_{a_0^0 \rightarrow \gamma\gamma}^2}{g_{f_0 \rightarrow \gamma\gamma}^2} = 0.77 \pm 0.48 \quad (27)$$

(where $M_{a_0} = M_{f_0} = 0.98 \text{ GeV}$ and an average error of 0.115 KeV for $\Gamma_{f_0 \rightarrow \gamma\gamma}$ have been used).

Large N_c results are still valid by invoking vector meson dominance, for which the decay into two photons occurs via two virtual vector mesons. Then, we first discuss the case $c_2^{\gamma\gamma} = 0$ (Solution A), where only the dominant contribution is considered. By using the mixing angle $\theta_S = 21.6^\circ$ (see Eq. (16)) we find the totally wrong ratio $g_{a_0^0 \rightarrow \gamma\gamma}^2/g_{f_0 \rightarrow \gamma\gamma}^2 = 724.7$, while the other option $\theta_S = -21.6^\circ$ implies $g_{a_0^0 \rightarrow \gamma\gamma}^2/g_{f_0 \rightarrow \gamma\gamma}^2 = 2.3$, which is still unacceptable when compared to the experimental result of (27). Even by modifying the scalar angle θ_S the situation is not improved; one finds a minimum for the ratio $g_{a_0^0 \rightarrow \gamma\gamma}^2/g_{f_0 \rightarrow \gamma\gamma}^2 = 1$ at $\theta_S = -70.5^\circ$. Such a value for the scalar mixing angle is however ruled out by the phenomenology of the strong decay analyzed in the previous section (a small mixing angle θ_S is common to all three analyzed scenarios and is in accord with the mass degeneracy of $a_0(980)$ and $f_0(980)$). Therefore, also the two-photon decay shows that the dominant decay mechanism, corresponding to a switch of q and \bar{q} analogous to Fig. 1.a, is not enough to describe the experimental data.

Let us then consider the case of a non-zero $c_2^{\gamma\gamma}$. We keep the scalar mixing angle θ_S as found in Sol. B and C respectively and we determine the ratio $c_2^{\gamma\gamma}/c_1^{\gamma\gamma}$ in order to reproduce the experimental result of Eq. (27)³

$$\text{Sol. B (Eq. (19), } \theta_S = -12.8^\circ) \Rightarrow \frac{c_2^{\gamma\gamma}}{c_1^{\gamma\gamma}} = 0.73 \quad (28)$$

$$\text{Sol. C (Eq. (21), } \theta_S = 35.8^\circ) \Rightarrow \frac{c_2^{\gamma\gamma}}{c_1^{\gamma\gamma}} = -1.04 \quad (29)$$

In both cases a large ratio $c_2^{\gamma\gamma}/c_1^{\gamma\gamma}$ is found; while in Sol. B it is still safely smaller than unity, in Sol. C a large (and negative < -1) ratio is obtained.

³Once the ratio is determined, one can fix the strength of $c_1^{\gamma\gamma}$ to reproduce $\Gamma_{f_0 \rightarrow \gamma\gamma}$ (Eq. (26)). The other width $\Gamma_{a_0^0 \rightarrow \gamma\gamma}$ is then also correctly described.

Furthermore, in Solution B we find a noticeable correspondence between the electromagnetic and strong transitions: $c_2^{\gamma\gamma}/c_1^{\gamma\gamma} = 0.73 \sim c_2/c_1 = 0.62$. The two-photon decay, which in the framework of vector meson dominance is mediated by two virtual vector mesons, differs from the two-pseudoscalar decay only in the final stage, therefore the contribution of the subleading diagram with respect to the leading one is naively expected to be of the same magnitude (and with the same sign). On the contrary in Solution C we have $c_2^{\gamma\gamma}/c_1^{\gamma\gamma} = -1.04 \ll c_2/c_1 = 0.89$: this fact would mean very different contributions of the subleading diagram in the decay amplitude into two vector mesons (then converting into two photons) from the corresponding transition into two pseudoscalar mesons. The composite approach used in this work does not allow for a more microscopic insights to deal rigorously with this issue, therefore this discussion does not represent a proof in favour of Sol. B. We simply limit to notice that within Sol. B one has $c_2^{\gamma\gamma}/c_1^{\gamma\gamma} \sim c_2/c_1$, which on the contrary does not take place in Sol. C.

The experimental situation concerning $\sigma \rightarrow 2\gamma$ is less clear; no average or fit is presented in [15], however two experiments listed in [15] find large $\gamma\gamma$ decay widths: 3.8 ± 1.5 keV and 5.4 ± 2.3 keV, respectively. In a footnote it is then state that these values could be assigned to $f_0(1370)$ (actually, in a older version of Particle Data Group [51] these values were assigned to the resonance $f_0(1370)$). It is not clear if the $\gamma\gamma$ signal comes from the high mass tail of the broad σ state or from $f_0(1370)$ (or even from both; in such case the experimental result would represent the sum, i.e. an upper limit for both resonances). Furthermore, the application of Eq. (23) is too naive for the broad σ state; in fact, due to the third power of the mass of the decaying resonance, the two-photon decay width is strongly influenced by a large width, especially from the right mass tail (the precise form of a mass distribution would be necessary for a more precise and quantitative analysis). Here we simply report the results for the ratio $g_{a_0^0 \rightarrow \gamma\gamma}^2/g_{\sigma \rightarrow \gamma\gamma}^2$ in the two scenarios: $g_{a_0^0 \rightarrow \gamma\gamma}^2/g_{\sigma \rightarrow \gamma\gamma}^2$ is 0.83 in Solution B (28) and 0.42 in Solution C (29). However, if a two-photon width between 3 and 5 keV should be entirely assigned to the σ -resonance as recently discussed in Ref. [52], the interpretation of the σ as a tetraquark state would be problematic, because in the four-quark scenario the $\gamma\gamma$ decay width of the σ would be of the same order of the $a_0^0(980)$ one (~ 0.3 keV), as the above reported coupling ratios $g_{a_0^0 \rightarrow \gamma\gamma}^2/g_{\sigma \rightarrow \gamma\gamma}^2$ suggest. Future work on the $\sigma \rightarrow \gamma\gamma$ transition is needed both theoretically and experimentally in order to clarify this crucial issue about light scalar mesons.

5 Summary and Conclusions

The Jaffe's four-quark states have appealing characteristics to be good candidates for the description of the scalar nonet below 1 GeV; this paper aimed to analyze this possibility by studying strong and the electromagnetic decays of scalar resonances.

We first considered the strong decays of the light scalar mesons below 1 GeV.

Beyond the OZI-superaligned decay, in which the scalar tetraquark state falls apart into two pseudoscalar mesons as depicted in Fig. 1.a, the next to leading order in the N_c expansion, which occurs with (only) one intermediate gluon as shown in Fig. 1.b, has been systematically taken into account for all decay coupling constants and presented in Tables 1, 2 and 3. The two decay mechanisms are described by corresponding terms in an effective composite interaction Lagrangian and are parametrized by two strength parameters c_1 and c_2 respectively.

As a first step we studied the case $c_2 = 0$, in which the diagram of Fig. 1.b is switched off. The large ratio $g_{f_0 \rightarrow \overline{K}K}^2 / g_{a_0 \rightarrow \overline{K}K}^2 = 2.15 \pm 0.40 > 1$ reported in the experimental analysis of [22] cannot be described because the theoretical ratio is ≤ 1 for $c_2 = 0$. We referred to the case $c_2 = 0$ as ‘Solution A’.

We then allowed for a non-zero ratio c_2/c_1 : by fitting c_2/c_1 and the scalar-isoscalar mixing angle θ_S to the three values reported in Eq. (15) deduced in the analysis of [22] and involving the $\overline{K}K$, $\pi\eta$ and $\pi\pi$ channels for the $a_0(980)$ and $f_0(980)$ states, a sizable ratio $c_2/c_1 = 0.62$ is obtained. The subdominant transition of Fig. 1.b is non negligible in the present analysis and improves the theoretical description of the mentioned decay modes of $a_0(980)$ and $f_0(980)$. The mixing angle $\theta_S = -12.8^\circ$ is small and negative: the bare components $\sigma_B \equiv “\overline{u}u\overline{d}d”$ and $f_B \equiv “\overline{s}s(\overline{u}u - \overline{d}d)”$ are out of phase in the physical state σ and in phase in the resonance $f_0(980)$. We called this scenario ‘Solution B’, which represents our preferred solution, as discussed in Sections 3 and 4.

Within Solution B one finds a very small ratio $g_{\sigma \rightarrow KK}^2 / g_{\sigma \rightarrow \pi\pi}^2 \sim 10^{-7}$, while the result reported in the analysis of Ref. [21] reads 0.6 ± 0.1 . Solution C has been then built by including this ratio when minimizing the χ -squared. As a result, agreement with [22] is obtained for the branching ratio $\overline{K}K/\pi\pi$, but the ratio $g_{f_0 \rightarrow \overline{K}K}^2 / g_{a_0 \rightarrow \overline{K}K}^2$ is found to be 1.11 within Solution C, which is, although larger than 1, clearly worsened with respect to Solution B. Future experimental check on $g_{\sigma \rightarrow KK}^2 / g_{\sigma \rightarrow \pi\pi}^2$ may help to clarify this point. The mixing angle in Sol. C is positive: $\theta_S = 31.8^\circ$, i.e. the bare components are in phase for σ and out of phase for $f_0(980)$. The sign difference of θ_S is responsible of such different results concerning the quantity $g_{\sigma \rightarrow KK}^2 / g_{\sigma \rightarrow \pi\pi}^2$.

The results of Solutions A, B and C are summarized in Table 4, where also other ratios of squared coupling constants are listed.

We then considered the two-photon decay of the scalar resonances. The diagrams for such transitions are similar to those of Fig. 1.a and 1.b but with photons instead of mesons as final states. The corresponding intensities are parametrized by $c_1^{\gamma\gamma}$ and $c_2^{\gamma\gamma}$ respectively.

The discussions follows the same line as before: the case $c_2^{\gamma\gamma} = 0$ (Sol. A) is analyzed first. The experimental result $\Gamma_{a_0 \rightarrow 2\gamma} / \Gamma_{f_0 \rightarrow 2\gamma} = g_{a_0 \rightarrow \gamma\gamma}^2 / g_{f_0 \rightarrow \gamma\gamma}^2 = 0.77 \pm 0.48$ cannot be obtained if $c_2^{\gamma\gamma} = 0$, thus again pointing to a non-zero contribution of the subleading diagram with one intermediate gluon.

We then analyzed Solutions B and C: by taking the scalar mixing angle θ_S from

Solution B or C the ratio $c_2^{\gamma\gamma}/c_1^{\gamma\gamma}$ has been determined in order to reproduce the experimental value $g_{a_0^2 \rightarrow \gamma\gamma}^2/g_{f_0^2 \rightarrow \gamma\gamma}^2 = 0.77 \pm 0.48$. In case B one has the noticeable correspondence $c_2^{\gamma\gamma}/c_1^{\gamma\gamma} \sim c_2/c_1$, that is the contribution of the subleading decay is similar (and with the same sign) in strong and electromagnetic transitions. This fact does not take place in Solution C where the two ratios are large but with opposite sign.

The interpretation of the light scalar states as tetraquark objects is a viable and interesting possibility. The inclusion of the subleading decay mechanism of Fig. 1.b improves the description of experimental data for both strong and electromagnetic transitions within our Solution B.

Future work is however needed: on a experimental side a clear experimental establishment of the resonance k and a better understanding of the parameters describing the broad states σ and k would constitute a decisive improvement.

We would like to mention possible future theoretical studies: the decays of heavier states, such as tensor mesons or scalar mesons above 1 GeV, into two light scalar mesons as $\sigma\sigma$, $kk\dots$ should be evaluated by explicitly taking into account the four-quark nature of the light scalars. Such a analysis would therefore extend and complete the ones in [9, 42]. In particular, the fact that the tensor meson nonet is well established and well known experimentally would offer a suitable environment for such a study. Furthermore, the two-body decay of excited pseudoscalar states (eventually mixed with a pseudoscalar glueball) would also constitute an interesting development. In the recent work of [53] attention is focused on electromagnetic decays of the type $S \rightarrow V\gamma$, which may also be helpful in disentangling the nature of the light scalar states below 1 GeV.

Acknowledgments

The author thanks J. Schaffner-Bielich for a careful reading of the manuscript and for very instructive comments. This research was supported by the Virtual Institute VH-VI-041 "Dense Hadronic Matter & QCD Phase Transitions" of the Helmholtz Association.

A Tetraquark scalar nonet

The wave function for a "good" diquark is [13]

$$|qq\rangle = |\text{space: } L = 0\rangle |\text{spin: } S = 0\rangle |\text{color: } \bar{\mathbf{3}}_C\rangle |\text{flavor: } \bar{\mathbf{3}}_F\rangle. \quad (30)$$

The state $|qq\rangle$ is antisymmetric by exchange of the two particles in accord with the Pauli principle; the parity quantum number is $P = (-1)^L = +1$. In the following we consider the flavor decomposition for a diquark (and for an antidiquark). To this end

we define the vector q such that $q^t = (u, d, s)$; the antisymmetric $\overline{\mathbb{3}}_F$ decomposition of a diquark is described by the antisymmetric matrix D :

$$D = \sqrt{\frac{1}{2}}(q_1 \cdot q_2^t - q_2 \cdot q_1^t) = \varphi_i A^i \quad (31)$$

where the matrices A^i are the three antisymmetric 3×3 real matrices of Eq. (6) and the quantities φ_i are given by

$$\varphi_1 = \sqrt{\frac{1}{2}}(u_1 d_2 - u_2 d_1) \equiv \sqrt{\frac{1}{2}}[u, d], \quad (32)$$

$$\varphi_2 = \sqrt{\frac{1}{2}}(u_1 s_2 - u_2 s_1) \equiv \sqrt{\frac{1}{2}}[u, s], \quad (33)$$

$$\varphi_3 = \sqrt{\frac{1}{2}}(d_1 s_2 - d_2 s_1) \equiv \sqrt{\frac{1}{2}}[d, s]. \quad (34)$$

The anti-diquark is then described by the matrix

$$D^\dagger = \overline{\varphi}_i (A^i)^\dagger = -\overline{\varphi}_i A^i \quad (35)$$

with $\overline{\varphi}_1 = \sqrt{1/2} [\overline{u}, \overline{d}]$, $\overline{\varphi}_2 = \sqrt{1/2} [\overline{u}, \overline{s}]$ and $\overline{\varphi}_3 = \sqrt{1/2} [\overline{d}, \overline{s}]$.

The matrix D has the following transformation properties:

$$SU(3)\text{-flavor:} \quad D \rightarrow U D U^t, \quad U \in SU(3), \quad (36)$$

$$P\text{-parity:} \quad D \rightarrow D, \quad (37)$$

$$C\text{-Charge Conjugation:} \quad D \rightarrow D^\dagger; \quad (38)$$

The flavor transformation (36), corresponding to $q \rightarrow Uq$, follows directly from the definition (31).

The matrix \mathcal{S} defined in Eq. (2) and entering in Eq. (3) is given by $\mathcal{S}_{ij} = \varphi_i \overline{\varphi}_j$.

In a generic Lagrangian term involving linear tetraquark scalar states (i.e. one matrix D and one matrix D^\dagger) one has a schematic form like

$$(\dots D \dots D^\dagger \dots) = \mathcal{S}_{ij} (\dots A^i \dots (A^j)^\dagger \dots) \quad (39)$$

where dots indicate operation with matrices, such as multiplication, traces, etc. The form on the l.h.s. is useful to check the $SU(3)$ -flavor transformations, while the form in the r.h.s. allows the calculations of the decay amplitudes (see Tables 1, 2, 3 and Appendix B). When describing the scalar \rightarrow two-pseudoscalar decay we then have the following possible flavor-invariant terms:

$$\begin{aligned} \mathcal{L}_{S \rightarrow PP} = & -c_1 \langle D \mathcal{P}^t D^\dagger \mathcal{P} \rangle + c_2 \langle D D^\dagger \mathcal{P}^2 \rangle + c_3 \langle D D^\dagger \mathcal{P} \rangle \langle \mathcal{P} \rangle \\ & + c_4 \langle D D^\dagger \rangle \langle \mathcal{P}^2 \rangle + c_5 \langle D D^\dagger \rangle \langle \mathcal{P} \rangle^2, \end{aligned} \quad (40)$$

where $\mathcal{P} = \frac{1}{\sqrt{2}} \sum_{i=0}^8 P^i \lambda_i$. The first two terms corresponds to the two diagrams of Fig. 1, i.e. to the last two terms of Eq. (3) (by applying the operation (39) the

equality is easily seen) described throughout all the work. The third term is also suppressed by a factor N_c only with respect to the OZI-superallowed decay, but the transition can occur with at least two transverse gluons as intermediate states attached to the pseudoscalar flavour-singlet state. The fourth and the fifth terms are further suppressed.

The Lagrangian $\mathcal{L}_{S \rightarrow PP}$ is clearly charge and parity invariant (we recall that $\mathcal{P} \rightarrow U\mathcal{P}U^\dagger$, $\mathcal{P} \rightarrow -\mathcal{P}$ and $\mathcal{P} \rightarrow \mathcal{P}^t$ under flavor, parity and charge conjugation transformations).

Formally the two-photon Lagrangian (22) can be obtained from Eq. (40) by replacing $\mathcal{P} \rightarrow QF_{\mu\nu}$, $c_i \rightarrow \hat{c}_i^{\gamma\gamma}$ (and then contracting the Lorentz indices). In virtue of $\langle Q \rangle = 0$ the first, the second and the fourth terms ‘survive’ the replacing; then, neglecting the latter we get the Lagrangian (22) (by invoking vector meson dominance, large N_c arguments can be applied also for the two-photon decays).

When considering the quadratic term for the scalar-tetraquark states care is needed; let us introduce an extra-index $a = 1, 2$ with $D^a = \varphi_i^a A^i$. The elements \mathcal{S}_{ij} (Eq. (2)) are formed by the two corresponding diquark φ_i^a and antidiquark $\bar{\varphi}_j^a$: $\mathcal{S}_{ij} = \varphi_i^a \bar{\varphi}_j^a$. Let us consider the flavor-invariant term $\langle D^1 (D^2)^\dagger \rangle \langle D^2 (D^1)^\dagger \rangle$; we aim to show that this is nothing else but $4 \langle \mathcal{S}^2 \rangle$ (proportional to the mass term of Eq. (3) in the flavour-symmetric limit):

$$\begin{aligned} \langle D^1 (D^2)^\dagger \rangle \langle D^2 (D^1)^\dagger \rangle &= \varphi_i^1 \bar{\varphi}_j^2 \varphi_k^2 \bar{\varphi}_l^1 \langle A^i A^j \rangle \langle A^k A^l \rangle \\ &= 4(\varphi_i^1 \bar{\varphi}_l^1)(\varphi_k^2 \bar{\varphi}_j^2) \delta_{ij} \delta_{kl} = 4\mathcal{S}_{il} \mathcal{S}_{li} = 4 \langle \mathcal{S}^2 \rangle. \end{aligned} \quad (41)$$

Then, in Eq. (3) modification from the flavor symmetric limit are parametrized by the matrix $\chi_S = \text{diag}\{\alpha, \beta, \beta\}$ and $\alpha < \beta$.

In Section 2.2 (Eq. (7)) we considered extra-terms in the scalar singlet-octet and singlet-singlet channels. The singlet-singlet channel, proportional to S_0^2 , is flavour-symmetric and corresponds to $\langle D^1 (D^1)^\dagger \rangle \langle D^2 (D^2)^\dagger \rangle$. The singlet-octet mixing introduced in Eq. (7) breaks flavour invariance. Here we notice that a flavour symmetric term, also including singlet-octet mixing (but affecting also the isovector and isodoublet states) can be constructed for the quadratic scalar sector:

$$\langle D^1 (D^1)^\dagger D^2 (D^2) \rangle = \mathcal{S}_{il} \mathcal{S}_{kl} \langle A^i A^j A^k A^l \rangle. \quad (42)$$

Further study on the mass sector for tetraquark scalar states including this term could be interesting.

B Strong coupling constants

We briefly recall the connection between the Lagrangian (3) and the coupling constants $g_{S \rightarrow P_1 P_2}^2$ entering in Eq. (12). After evaluating the traces, the Lagrangian

(3) can be rewritten as a sum over all the decay channels $S \rightarrow P_1 P_2$, where $S = \{a_0^\pm, a_0^0, k^\pm, k_0, \bar{k}_0, \sigma, f_0\}$ and $P = \{\pi^\pm, \pi^0, K^\pm, K_0, \bar{K}_0, \eta, \eta'\}$:

$$\begin{aligned}
\mathcal{L}_{S \rightarrow PP} &= c_1 \mathcal{S}_{ij} \langle A^i \mathcal{P}^t A^j \mathcal{P} \rangle - c_2 \mathcal{S}_{ij} \langle A^i A^j \mathcal{P}^2 \rangle \\
&= (\sqrt{2}c_1 + \frac{c_2}{\sqrt{2}})(a_0^0 K^- K^+ - K^0 \bar{K}^0) + (c_1 + c_2)(2\sigma_B \pi^+ \pi^- + \sigma_B (\pi^0)^2) + \dots \\
&= \sum_{S, P_1, P_2} \lambda_{S \rightarrow P_1 P_2} S P_1 P_2, \tag{43}
\end{aligned}$$

where in the second line we wrote the a_0^0 to $\bar{K}K$ and the σ_B to $\pi\pi$ couplings explicitly; they serve as illustrative examples of the adopted conventions. The coupling constants at this stage (without sum/average over isomultiplets) are simply given by $g_{S \rightarrow P_1 P_2} = s \cdot \lambda_{S \rightarrow P_1 P_2}$, where $s = 2/\sqrt{2} = \sqrt{2}$ when $P_1 = P_2$, 1 otherwise.

We have, for instance, $g_{a_0^0 \rightarrow K^+ K^-} = (\sqrt{2}c_1 + \sqrt{1/2}c_2)$, $g_{a_0^0 \rightarrow \bar{K}^0 K^0} = -(\sqrt{2}c_1 + \sqrt{1/2}c_2)$, $g_{\sigma_B \rightarrow \pi^+ \pi^-} = 2(c_1 + c_2)$, $g_{\sigma_B \rightarrow \pi^0 \pi^0} = \sqrt{2}(c_1 + c_2)$. Notice that by plugging these coupling constants into (12) we get the partial decay width for the corresponding channel, such as $\Gamma_{a_0^0 \rightarrow K^+ K^-}$.

Let us then group the final states in corresponding isomultiplets: $P = \{\pi, K, \eta, \eta'\}$. One has to perform the sum over the members of the isomultiplets, for instance:

$$g_{a_0^0 \rightarrow \bar{K}K}^2 = g_{a_0^0 \rightarrow K^+ K^-}^2 + g_{a_0^0 \rightarrow \bar{K}^0 K^0}^2 \rightarrow g_{a_0^0 \rightarrow \bar{K}K} = \sqrt{2}g_{a_0^0 \rightarrow K^+ K^-} \tag{44}$$

$$g_{\sigma_B \rightarrow \pi\pi}^2 = g_{\sigma_B \rightarrow \pi^+ \pi^-}^2 + g_{\sigma_B \rightarrow \pi^0 \pi^0}^2 \rightarrow g_{\sigma_B \rightarrow \pi\pi} = \sqrt{\frac{3}{2}}g_{\sigma_B \rightarrow \pi^+ \pi^-} \tag{45}$$

The sign of the resulting coupling constant can be chosen arbitrarily for the isotriplet and isodoublets a_0 and k states. In the a_0^0 to $\bar{K}K$ case we chose the sign of the charged decay channel $K^+ K^-$ (which is opposite to the $\bar{K}^0 K^0$ one); Table 1 is compiled following this convention. This however does not affect the decay rates expressed in (12). Care is needed in the scalar-isoscalar sector because of mixing occurring in Eq. (14), such as $g_{\sigma_B \rightarrow \pi\pi}$: the sign of $g_{\sigma_B \rightarrow \pi\pi}$ is taken to be the same as $g_{\sigma_B \rightarrow \pi^+ \pi^-}$ and $g_{\sigma_B \rightarrow \pi^0 \pi^0}$. In the scalar-isoscalar sector the various contributions to the sum over final isomultiplets have the same overall sign, thus making the definition unambiguous. Table 2 and 3 follow this convention.

As a last step an average over the initial isospin multiplets is performed, that is we consider $S = \{a_0, k, \sigma, f_0\}$. For instance, $g_{a_0 \rightarrow \bar{K}K}^2$ is given by:

$$g_{a_0 \rightarrow \bar{K}K}^2 = \frac{1}{3} \left(g_{a_0^0 \rightarrow \bar{K}K}^2 + g_{a_0^+ \rightarrow \bar{K}K}^2 + g_{a_0^- \rightarrow \bar{K}K}^2 \right) = g_{a_0^0 \rightarrow \bar{K}K}^2. \tag{46}$$

The terms of the average are equal (this is true for each decay of a_0 and k ; for σ and f_0 no average is needed).

References

- [1] C. Amsler and N. A. Tornqvist, Phys. Rept. **389**, 61 (2004).
- [2] F. E. Close and N. A. Tornqvist, J. Phys. G **28**, R249 (2002) [arXiv:hep-ph/0204205];
- [3] P. Minkowski and W. Ochs, Nucl. Phys. Proc. Suppl. **121**, 123 (2003) [arXiv:hep-ph/0209225];
- [4] C. Amsler and F. E. Close, Phys. Lett. B **353**, 385 (1995) [arXiv:hep-ph/9505219]; C. Amsler and F. E. Close, Phys. Rev. D **53**, 295 (1996) [arXiv:hep-ph/9507326].
- [5] W. J. Lee and D. Weingarten, Phys. Rev. D **61**, 014015 (2000) [arXiv:hep-lat/9910008];
- [6] M. Strohmeier-Presicek, T. Gutsche, R. Vinh Mau and A. Faessler, Phys. Rev. D **60**, 054010 (1999) [arXiv:hep-ph/9904461].
- [7] F. E. Close and A. Kirk, Eur. Phys. J. C **21**, 531 (2001) [arXiv:hep-ph/0103173].
- [8] F. Giacosa, T. Gutsche and A. Faessler, Phys. Rev. C **71**, 025202 (2005) [arXiv:hep-ph/0408085].
- [9] F. Giacosa, T. Gutsche, V. E. Lyubovitskij and A. Faessler, Phys. Rev. D **72**, 094006 (2005) [arXiv:hep-ph/0509247].
F. Giacosa, T. Gutsche, V. E. Lyubovitskij and A. Faessler, Phys. Lett. B **622**, 277 (2005) [arXiv:hep-ph/0504033].
- [10] M. B. Voloshin and L. B. Okun, JETP Lett. **23**, 333 (1976) [Pisma Zh. Eksp. Teor. Fiz. **23**, 369 (1976)]. K. Maltman and N. Isgur, Phys. Rev. Lett. **50**, 1827 (1983). K. Maltman and N. Isgur, Phys. Rev. D **29**, 952 (1984).
- [11] N. A. Tornqvist, Phys. Rev. Lett. **67**, 556 (1991).
N. A. Tornqvist, Z. Phys. C **61**, 525 (1994) [arXiv:hep-ph/9310247].
T. E. O. Ericson and G. Karl, Phys. Lett. B **309**, 426 (1993).
- [12] R. L. Jaffe, Phys. Rev. D **15** (1977) 267.
R. L. Jaffe, Phys. Rev. D **15** (1977) 281.
R. L. Jaffe and F. E. Low, Phys. Rev. D **19**, 2105 (1979).
- [13] R. L. Jaffe, Phys. Rept. **409** (2005) 1 [Nucl. Phys. Proc. Suppl. **142** (2005) 343] [arXiv:hep-ph/0409065].

- [14] L. Maiani, F. Piccinini, A. D. Polosa and V. Riquer, Phys. Rev. Lett. **93** (2004) 212002 [arXiv:hep-ph/0407017].
- [15] S. Eidelman *et al.* [Particle Data Group Collaboration], Phys. Lett. B **592**, 1 (2004).
- [16] E. Van Beveren, T. A. Rijken, K. Metzger, C. Dullemond, G. Rupp and J. E. Ribeiro, Z. Phys. C **30** (1986) 615.
- [17] S. Ishida, M. Ishida, T. Ishida, K. Takamatsu and T. Tsuru, Prog. Theor. Phys. **98** (1997) 621 [arXiv:hep-ph/9705437].
- [18] D. Black, A. H. Fariborz, F. Sannino and J. Schechter, Phys. Rev. D **58** (1998) 054012 [arXiv:hep-ph/9804273].
- [19] E. M. Aitala *et al.* [E791 Collaboration], Phys. Rev. Lett. **86** (2001) 765 [arXiv:hep-ex/0007027].
- [20] D. V. Bugg, arXiv:hep-ex/0510014.
- [21] D. V. Bugg, arXiv:hep-ph/0603089.
- [22] D. V. Bugg, arXiv:hep-ex/0603023.
- [23] M. Ablikim *et al.* [BES Collaboration], Phys. Lett. B **598** (2004) 149 [arXiv:hep-ex/0406038].
- [24] A. Dobado and J. R. Pelaez, Phys. Rev. D **56** (1997) 3057 [arXiv:hep-ph/9604416].
- [25] J. A. Oller and E. Oset, Nucl. Phys. A **620** (1997) 438 [Erratum-ibid. A **652** (1999) 407] [arXiv:hep-ph/9702314].
- [26] J. A. Oller, E. Oset and J. R. Pelaez, Phys. Rev. D **59** (1999) 074001 [Erratum-ibid. D **60** (1999) 099906] [arXiv:hep-ph/9804209].
- [27] J. R. Pelaez, Phys. Rev. Lett. **92** (2004) 102001 [arXiv:hep-ph/0309292].
- [28] J. R. Pelaez, Mod. Phys. Lett. A **19** (2004) 2879 [arXiv:hep-ph/0411107].
- [29] M. G. Alford and R. L. Jaffe, Nucl. Phys. B **578** (2000) 367 [arXiv:hep-lat/0001023].
- [30] F. Okiharu, H. Suganuma, T. T. Takahashi and T. Doi, arXiv:hep-lat/0601005.
- [31] A. H. Fariborz, R. Jora and J. Schechter, Phys. Rev. D **72** (2005) 034001 [arXiv:hep-ph/0506170]. A. H. Fariborz, Int. J. Mod. Phys. A **19** (2004) 2095 [arXiv:hep-ph/0302133].

- [32] M. Napsuciale and S. Rodriguez, Phys. Rev. D **70** (2004) 094043 [arXiv:hep-ph/0407037].
- [33] S. Weinberg, Physica A **96** (1979) 327; J. Gasser and H. Leutwyler, Annals Phys. **158**, 142 (1984); Nucl. Phys. B **250** (1985) 465.
- [34] S. Scherer, arXiv:hep-ph/0210398.
- [35] G. Ecker, J. Gasser, A. Pich and E. de Rafael, Nucl. Phys. B **321**, 311 (1989); G. Ecker, J. Gasser, H. Leutwyler, A. Pich and E. de Rafael, Phys. Lett. B **223**, 425 (1989).
- [36] V. Cirigliano, G. Ecker, H. Neufeld and A. Pich, JHEP **0306** (2003) 012 [arXiv:hep-ph/0305311].
- [37] E. P. Venugopal and B. R. Holstein, Phys. Rev. D **57**, 4397 (1998) [arXiv:hep-ph/9710382].
- [38] J. Schaffner-Bielich and J. Randrup, Phys. Rev. C **59** (1999) 3329 [arXiv:nucl-th/9812032].
J. Schaffner-Bielich, Phys. Rev. Lett. **84** (2000) 3261 [arXiv:hep-ph/9906361].
- [39] E. Klempt, arXiv:hep-ex/0101031.
- [40] M. Benayoun, L. DelBuono and H. B. O'Connell, Eur. Phys. J. C **17** (2000) 593 [arXiv:hep-ph/9905350].
- [41] C. Bini, eConf **C030626** (2003) FRAT08 [arXiv:hep-ex/0308046].
- [42] F. Giacosa, T. Gutsche, V. E. Lyubovitskij and A. Faessler, Phys. Rev. D **72** (2005) 114021 [arXiv:hep-ph/0511171].
- [43] V. Baru, J. Haidenbauer, C. Hanhart, A. Kudryavtsev and U. G. Meissner, Eur. Phys. J. A **23** (2005) 523 [arXiv:nucl-th/0410099].
- [44] S. M. Flatte, Phys. Lett. B **63** (1976) 228.
- [45] M. Ablikim *et al.* [BES Collaboration], Phys. Lett. B **607** (2005) 243 [arXiv:hep-ex/0411001].
- [46] M. Ablikim *et al.* [BES Collaboration], Phys. Lett. B **633** (2006) 681 [arXiv:hep-ex/0506055].
- [47] F. Ambrosino *et al.* [KLOE Collaboration], Phys. Lett. B **634** (2006) 148 [arXiv:hep-ex/0511031].
- [48] J. A. Oller, Nucl. Phys. A **714** (2003) 161 [arXiv:hep-ph/0205121].

- [49] J. E. Palomar, L. Roca, E. Oset and M. J. Vicente Vacas, Nucl. Phys. A **729** (2003) 743 [arXiv:hep-ph/0306249].
- [50] N. N. Achasov, S. A. Devyanin and G. N. Shestakov, Phys. Lett. B **96** (1980) 168.
- [51] D. E. Groom *et al.* [Particle Data Group Collaboration], Eur. Phys. J. C **15**, 1 (2000).
- [52] M. R. Pennington, arXiv:hep-ph/0604212.
- [53] Y. Kalashnikova, A. Kudryavtsev, A. V. Nefediev, J. Haidenbauer and C. Hanhart, Phys. Rev. C **73** (2006) 045203 [arXiv:nucl-th/0512028].

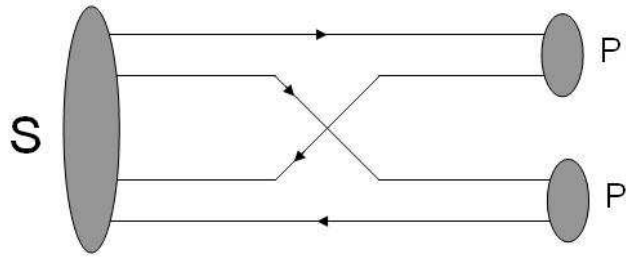


Fig 1.a

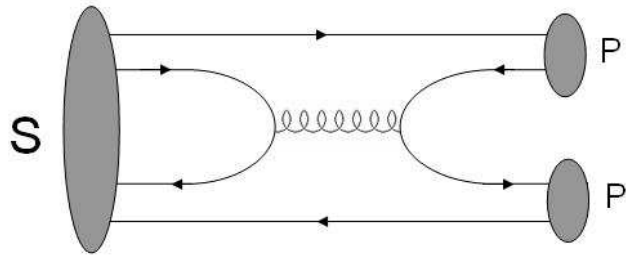


Fig 1.b

Figure 1: Dominant (1.a) and subdominant (1.b) contributions to the transition amplitudes of a scalar tetraquark state into two pseudoscalar mesons.